A98-31620 ICAS-98-4,11,3

A LIGHTWEIGHT CONCEPT FOR AERODYNAMIC SURFACES WITH VARIABLE CAMBER

Lucio Flavio Campanile

Holger Hanselka

DLR, Institute of Structural Mechanics, Braunschweig (Germany)

Abstract

In this work a new concept for an aerodynamic surface with variable camber is presented. The changes with respect to the traditional structural design are kept to a minimum. The conventional rib, in charge of the aerodynamic section's shape stability, is replaced by a „camber-flexible" rib. In contrast to the traditional rib, the camber-flexible rib allows in-plane deformations. However, due to the rib's special construction, these occur mainly as changes in the section camber. The section camber can be selected and controlled under load by an appropriate actuator system.

The camber-flexible rib is realized with a closed shell *(belt)*, reinforced by in-plane stiffeners *(spokes)*. The spokes' main task is to restrain the rib's in-plane flexibility in such a way, that undesired deformations can be avoided. The spokes are connected to the belt by hinges and the whole section stiffness of the rib is provided by the belt's bending stiffness.

Together with the description of the new structure, with some options for the integration in a real aerodynamic surface, some simulation and experimental results on a prototype are presented in the paper.

Introduction

The aerodynamic forces on a lifting surface depends strongly on its geometry. Full control of aerodynamic forces would imply full geometrical adaptability. A look to bird flight conveys entire, continuous geometry control as the way chosen by nature to keep aerodynamics under control and maximize flight efficiency and safety.

Lifting surface geometry of airplanes is controlled by very few degrees of freedom, through the relative position of rigid surfaces. Of course, this drastically restricts efficiency and maneuverability. For most part of its service, the aircraft's geometrical configuration is far from the optimal one. Realizing lifting surfaces with extensive geometry control would release a huge improvement potential concerning aircraft productiveness, reliability and operational flexibility.

The advantages of extensive geometrical adaptability of lifting surfaces are known since the infancy of aviation's history. Even the Wright Brothers in their first flight made use of structural flexibility in order to induce camber changes for control purposes[1].

Camber variation is not only widely recognized as a very effective way of influencing lift but also regularly used in other application fields of aerodynamics, like sailing[2]. Its use in aeronautics was evidently not possible up to now due to the absence of opportune structural design solutions.

The first inventions concerning lifting surfaces with variable geometry date from the thirties[3-5]. Fifty years later the research activity in this field became very intensive, as documented by the large number of patents[6-9] and papers[1,10-12] on this topic. As a rule, the proposed approach achieve the desired geometrical adaptability by means of complex mechanisms. In most cases, such a radical change in the design of the aerodynamic surface is required, that some structural elements are no longer able to perform their typical load-carrying function. Hence they must be supplemented by additional elements, which results in a considerable increase in weight. Many concepts do not preserve the skin's

structural function; typically, the skin's profile has to be opened, resulting in a massive loss of torsional stiffness.

The aircraft industry, with its extreme reliability standard, is evidently not willing to accept solutions which require revolutionary changes of the established and well-proven airfoil design. Only a lightweight-optimized structural concept, which preserves the classical wing design philosophy, has a chance to be adopted in the future aircraft generation.

Advantages of aerodynamic surfaces with variable camber

The benefits of variable camber for an aircraft wing were pointed out by many authors [1,10-13].

The main advantages can be summarized as follows:

- increase of aerodynamic efficiency (L/D ratio) by up to 9%,
- extended buffet boundaries by up to 15% and
- reduction of wing root bending moments by up to 12%,

resulting in reduction of fuel consumption and structural weight as well as improved maneuverability and operational flexibility.

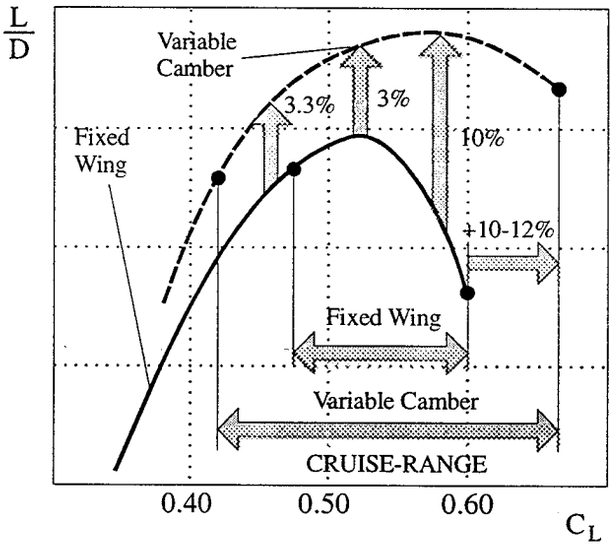

FIGURE 1 Effect of variable camber on aerodynamic efficiency [10,11]

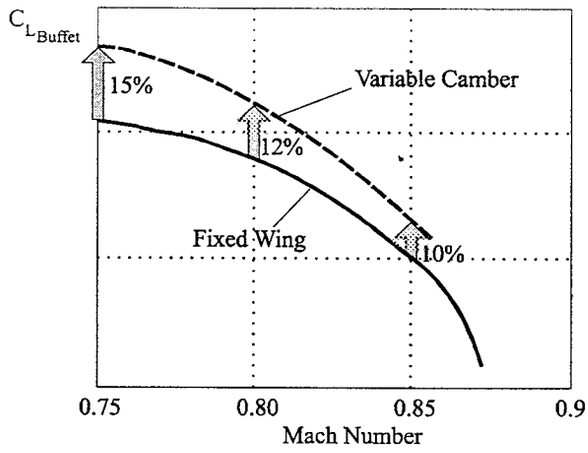

FIGURE 2 Effect of variable camber on buffet boundaries [10,11].

The effect of variable camber on aerodynamic efficiency and buffet boundaries is shown in Figures 1 and 2.

Design requirements

Most of the research projects on the topic of variable camber airfoil see as a first goal the modification of the leading-edge and trailing-edge regions. This would allow to investigate and check the feasibility of the different solution without requiring modifications of the wing box.

The target of the research work reported in this paper is the realization of a landing flap with variable camber for a transport aircraft. The reference flap structure is represented by the outboard flap of the Airbus A340 aircraft.

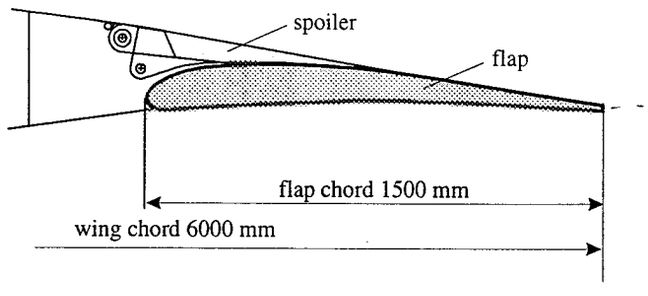

FIGURE 3 A340-flap representative section

The flap has a spanwise length of 10.21 m; the chord ranges from 1.24 to 1.79 m. Figure 3 shows the representative section of the flap which will be used a reference section later in this paper.

The design load distributions are reported in Figure 4. The load results from the pressure distributions on the upper and on the lower side which are assumed to be of equal intensity and opposite sign. The strength design load corresponds to the maneouver load with a safety coefficient of 1.5.

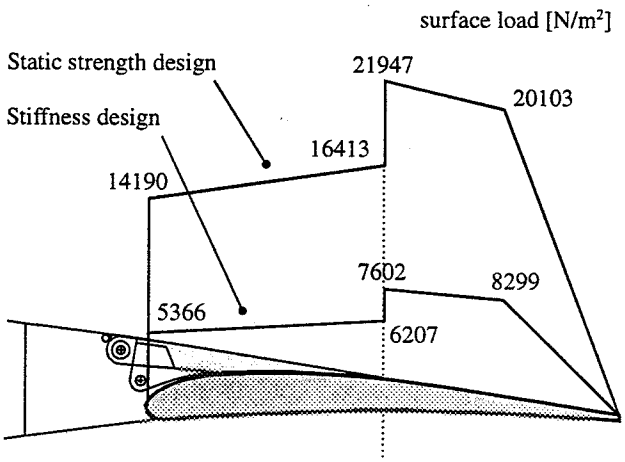

FIGURE 4 Design load distributions

The required geometrical adaptability is shown in Figure 5. The camber-flexible region extends for ca. 40% of the flap chordwise length, corresponding to 10% of the wing chord. The level of cambering or de-cambering is expressed in degrees, taking the beginning of the flexible zone as a reference. The desired maximum deflection of ±5° corresponds to a vertical displacement at the trailing edge of ca. 50 mm.

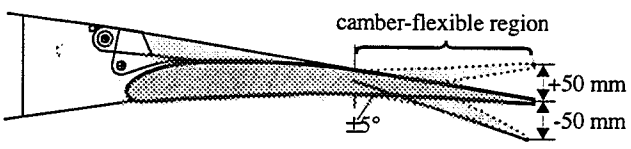

FIGURE 5 Required geometrical adaptability

The "belt rib" basic idea

The structural design of a modern airplane constitutes a masterpiece of structural optimization. Due to the essential need to contain weight, every structural element is designed in a way that maximizes its load-carrying capabilities per unit weight. The most representative example of this design philosophy is the typical wing structure (Figure 6), constituted by spars, ribs, stringer and skin, also widely adopted for other aerodynamic surfaces, like control surfaces and high-lift devices.

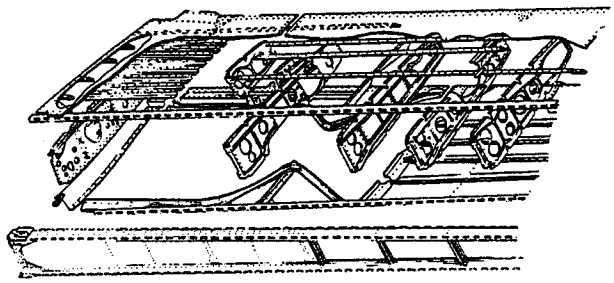

FIGURE 6 Classical airfoil design [15]

Due to such optimized structure, aerodynamic devices are able to fulfill high strength and stiffness requirements in spite of low weight. As soon as stiffness requirements are concerned, the need of containing displacements and deformations within defined limits assumes an essential importance for aircraft structures. Since aerodynamic forces depends directly on the wing geometry, undesired displacements can compromise the aircraft's controllability and cause fatal aeroelastic phenomena.

In particular, the classical wing guarantees a very high degree of shape stability of the airfoil section. The structural elements which are in charge of such stability are the ribs, which are usually built as plates. Of course, a wing structure with variable camber cannot be realized with classical ribs. On the other side, simply removing the ribs would introduce undesired flexibility, e. g. concerning the section thickness. Therefore, a new kind of rib must be designed, which allows camber changes within given limits and leaves the remaining in-plane stiffness properties widely unchanged.

The new rib should interface to the remaining structural elements in such a way, that no essential changes in their structural function are required. Only in this way the degree of structural optimization can be kept at a high level.

In its basic form (Figure 7), the new rib structure which is presented in this work *(belt rib)* consists in a closed shell *(belt)* reinforced by in-plane stiffeners *(spokes)*. The spokes are connected to the belt by hinges[16].

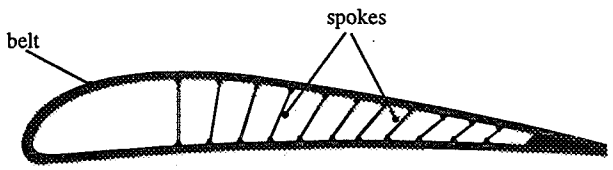

FIGURE 7 - Belt rib

The belt rib is loaded by in-plane forces applied on the belt. Its *in-plane flexibility* defines the belt's shape changes as a function of the load.

Since they are not subject to forces on their length, the spokes are loaded in a pure tension-compression mode. As a rule, their longitudinal flexibility give no essential contribution to the in-plane flexibility of the belt rib, so that they can be assumed to be rigid. In this case, the in-plane flexibility of the belt rib is defined by the belt's bending flexibility and the spokes' configuration.

For a belt with given external contour, constant thickness and homogeneous material, the deformation mode is essentially defined by the spokes' configuration. Choosing an opportune configuration makes possible to induce a "qualified" flexibility of the rib, which mainly allows camber changes.

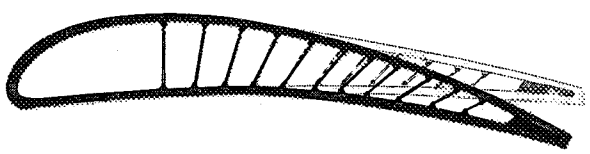

FIGURE 8 - Typical deformation of the belt rib

The spokes' configuration shown in Figure 7 was chosen to this purpose. The aerodynamic section corresponds to the above mentioned high-lift device. A typical deformation mode for the considered structure is shown in Figure 8.

Due to the "qualified" flexibility, the load distribution has only a secondary influence on the belt's deformation. For the same reason, the selection of the desired camber can be achieved with a reduced number of control forces.

The belt-rib flap structure

Figure 9 shows the structural assembly of a flap based on the belt-rib concept.

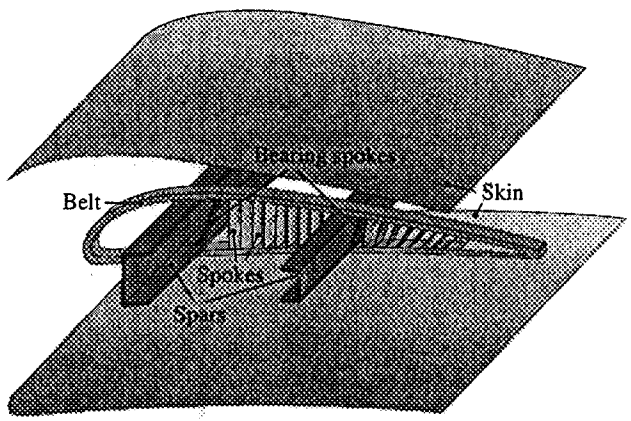

FIGURE 9 - Belt-rib flap assembly

The lower part of the spars is directly connected to the belt. The connection between the belt's upper side and the spars is realized through two major spokes (bearing spokes). The skin is bound to the belt and follows its deformation pattern.

In Figure 10 the spokes configuration of the belt rib is shown. This configuration was chosen in order to allow camber changes mainly in the trailing edge region, behind the rear spar (see Figure 11).

Actuator forces for camber control can be applied in different ways. A classical stroke actuator can exert a force between one spar and the corresponding bearing spoke (Figure 12, a).

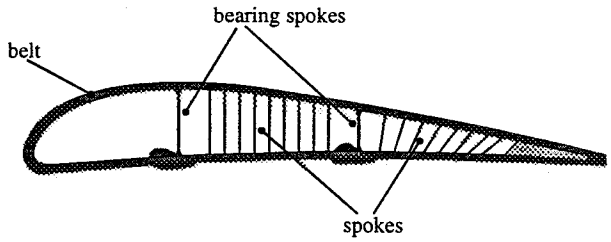

FIGURE 10 - Spokes configuration of the belt rib

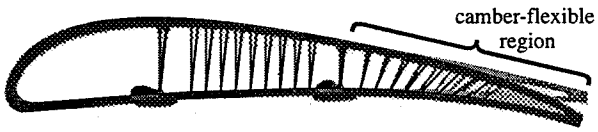

FIGURE 11 - Belt-rib's deformation mode

Loading through forces between opposite hinges of the bearing spokes (Figure 12, b) would be suitable for actuation by active wires (e. g. Shape Memory Alloy wires). A leading and/or trailing-edge actuation (Figure 12, c) could be realized not only mechanically but also through aerodynamic actuation devices. Active hinges can also be used, which directly influence the angle between one or more spokes and the belt (Figure 12, d). In this case however, the corresponding spokes would be loaded by a bending moment and not only longitudinally as in the standard case and should be consequently dimensioned. Embedded active material, like Shape Memory Alloys or piezoelectric materials, can also be used in order to directly induce the desired camber variation in the belt (Figure 12, e). An attractive advantage of using induced-strain actuators in the camber–flexible region is the loading reduction of passive material.

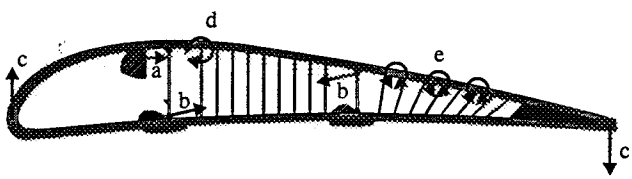

FIGURE 12 - Actuator options

Finite-Element Simulations

The feasibility of the new flap structure design was firstly checked by means of FEM-Simulations of the belt rib. The model geometry and material properties were chosen in order to match the design requirements of the A340-flap.

The section geometry is the same as reported in Figure 1. The belt was modeled with constant cross section properties. The cross section bending stiffness has a value of 437.5 Nm^2, which corresponds for example to a 50 mm wide and 10 mm thick belt made of aluminum alloy (E= 70 GPa). The skin contribution to the bending stiffness is not considered here and will be taken into account later in this section.

The distance between the ribs on the span direction, which determines the aerodynamic load on the single rib, amounts to 500 mm. From the aerodynamic load distributions which are reported in Figure 4 the load per unit length on the rib can be calculated (Figure 13).

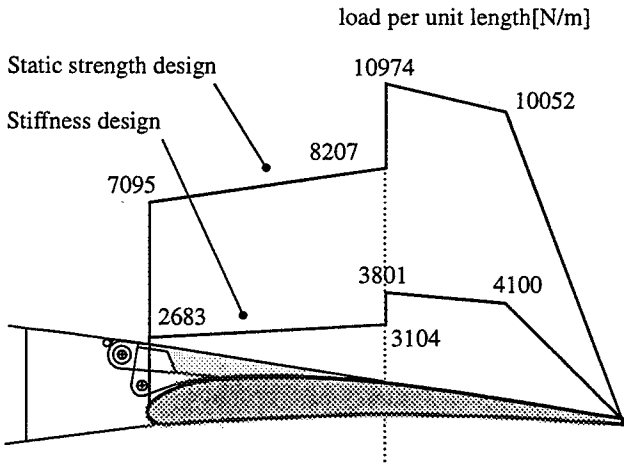

FIGURE 13 - Design load on the rib

A first simulation result concerns the deformation mode. The actuator force was applied horizontally at the upper node of the element representing the front bearing spoke. Figure 14 shows the belt

cambering and de-cambering under actuator force without external load. The actuator force amounts to ±2600 N, the actuator stroke ±9.3 mm for a camber variation corresponding to a vertical trailing edge displacement of ±46.7 mm.

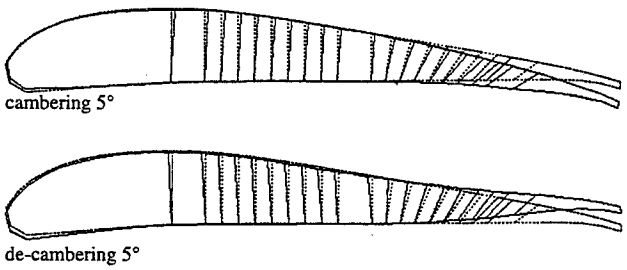

FIGURE 14 - FEM results: deformation mode (actuator load)

In order to check the fulfillment of the stiffness requirements the deformation under aerodynamic load (stiffness design) with blocked actuator is to be considered. The corresponding simulation results are shown in Figure 15. The graph scale is stretched; the maximum displacement in the trailing edge region has a value of 2.7 mm.

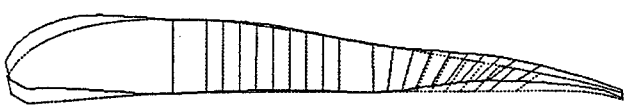

FIGURE 15 - FEM results: deformation under aerodynamic load

For correct actuator design, the maximum actuator force is to be computed. Since the aerodynamic load tends to de-camber the section, the maximum actuator force is necessary for maximum camber increase under aerodynamic load (strength design). The resulting actuator force is ca. 6800 N.

For the purpose of strength evaluation, the strain distribution for the heaviest loading case (strength design x 1.5 safety coefficient) was computed. The maximum strain, with a value of ca. 0.25 %, does not reach a critical level.

As mentioned above, the presented results do not take into account the stiffening effect provided by the skin. The skin stiffening effect is expected to be equivalent to an increase in the belt's bending stiffness. Therefore the belt's thickness in the final assembly can be reduced by an opportune factor resulting in the same in-plane stiffness.

A theoretical estimate of the thickness reduction factor in the case that the belt and the skin have the same Young's modulus can be obtained assuming the system belt-skin behaving like a T-beam.

The second moment of area for the belt-skin system can be expressed as follows (with some approximations admissible for small skin/belt thickness ratio):

$$I = \frac{bh^3}{3} + (ls - bh)\frac{b^2h^4}{4(bh+ls)^2}, \qquad (1)$$

with the notations of Figure 16.

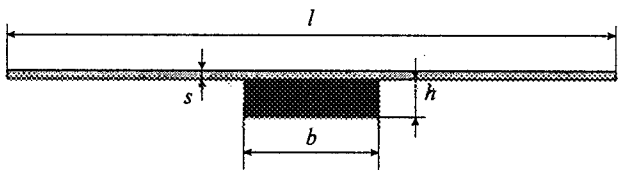

FIGURE 16 – Cross section of the belt-skin system

Rearranging Equation (1) leads to

$$I = \frac{bh^3}{12}\left(4 + 3\frac{(\xi - 1)}{(\xi + 1)^2}\right), \quad \xi = \frac{ls}{bh}. \qquad (2)$$

The expression in parenthesis is the skin "stiffening factor". With the above mentioned data $l = 500\,\text{mm}$, $h = 5\,\text{mm}$, $b = 50\,\text{mm}$ and with skin thickness $s = 1\,\text{mm}$ is $\xi = 2$ and the stiffening

factor amounts to 4,33. That means that reducing the belt thickness by factor

$$\alpha = \sqrt[3]{\frac{1}{4{,}33}} = 0.614\,, \qquad (3)$$

would lead to the same in-plane stiffness for the assembled rib.

The thickness reduction contributes to a reduction in maximum strain; at the same time however, the neutral axis shifts toward the skin, causing an increase in maximum strain. The strain correction factor assumes the following expression:

$$\beta = 2\left(4+3\frac{(\xi-1)}{(\xi+1)^2}\right)^{-1/3} - \frac{1}{1+\xi}\,. \qquad (4)$$

For the above mentioned case $\xi = 2$ results $\beta = 0.893$.

The belt-rib prototype

A first experimental check of the new structural concept was carried out on a belt-rib prototype (Figure 17).

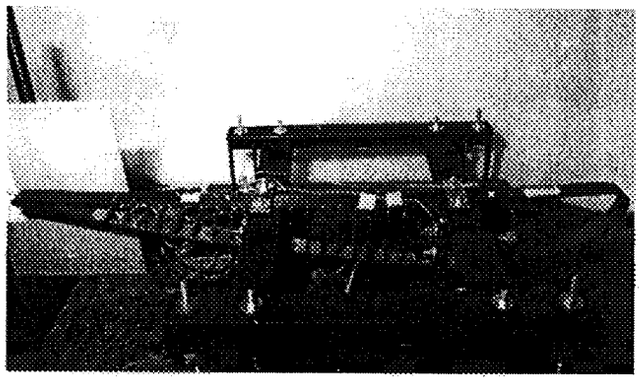

FIGURE 17 - The belt-rib prototype

The prototype was realized on the scale of 1:2 compared to the FEM-Model geometry. A 1:2 scale factor for length and displacement implies a 1:4 scale factor for forces; stresses and strains remain unchanged.

The belt and the spokes (with exception of the bearing spokes) were realized in carbon fiber/epoxy resin composite. The Young's modulus of the belt material in the direction of interest (tangential to the belt contour) was about 140 GPa. In order to obtain the same bending stiffness, the belt thickness was reduced by a factor 0.8, which corresponds to ca. factor 0.5 in the second moment of area and compensates for the higher Young's modulus. The maximum strain in the belt, which for a given local curvature change is proportional to the thickness, is reduced by factor 0.8 as well.

The remaining structural elements (hinges, bearing spokes, spars) were of steel.

The belt rib was activated by a force between front spar and front bearing spoke (corresponding to the actuation option in Figure 12a) which was exerted by a simple screw actuator.

Experimental test

The deformation mode for maximum cambering and de-cambering (trailing edge vertical displacement $\pm$ 2.5 mm, corresponding to $\pm$ 5 mm on a full scale) is shown in Figure 18.

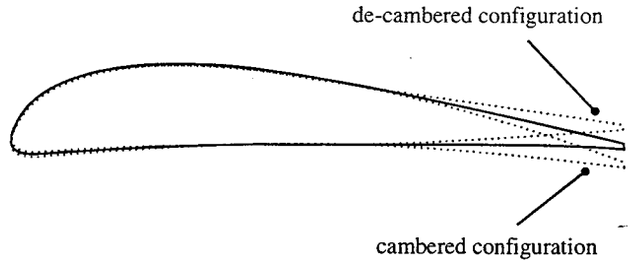

FIGURE 18 - Measured deformation mode

Strain was measured by means of strain gauges in some different positions. Among the chosen measuring points in the trailing edge region the

maximum strain level occurs in the position shown in Figure 19. The strain in this point, which is reported in Figure 20 as a function of the trailing edge displacement, shows a linear pattern.

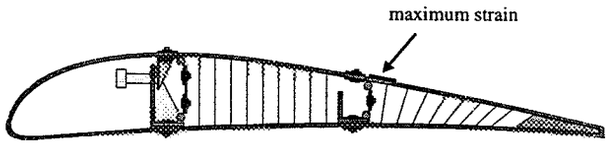

FIGURE 19 - Prototype section; maximum strain position

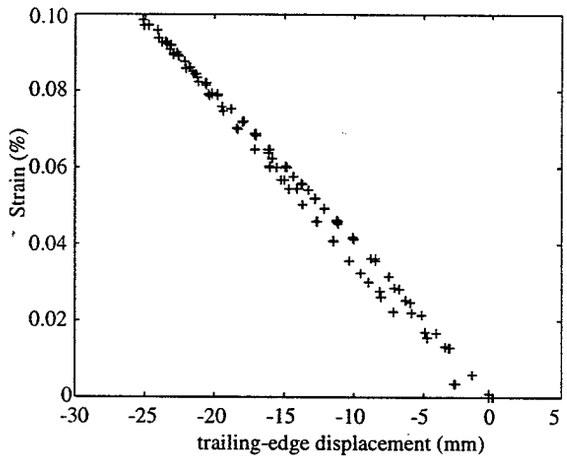

FIGURE 20 - Strain as a function of trailing-edge displacement

The FEM computations for the case of pure actuator force provide in the considered point a maximum strain value of ca. 0.14%. Taking into account the above mentioned correction factor (0.8), a value of 0.11% strain is expected as maximum value. The measured value of 0.099 show an good agreement in consideration of the possible error sources (material properties and geometry estimation, use of a simple FEM-Model with surface elements and no geometric non-linearity, etc.).

Design parameters and structural improvement potential

The structural design process of a belt rib structure based on a given geometrical adaptability is primarily ruled by the conflict between the stiffness and the strength requirements.

Producing the desired camber variation in a classical wing structure would obviously require enormous actuator forces. Even if the needed forces were available, the structure would collapse due to the huge strain level. On the other side rendering the structure very flexible would be ideal for the purpose of geometrical adaptation but would be no practicable solution due to the loss of shape stability under external load.

The stiffness requirements set a lower limit for the in-plane stiffness of the belt-rib structure and consequently for the belt's bending stiffness.

On the other side, the maximum local camber increase sets an upper limit for the belt's thickness, if a defined strain level is not to be exceeded.

For a given material, the minimum bending stiffness condition defines the following relationship between width b and thickness h of the belt:

$$b = 12\frac{I}{h^3}, \qquad (5)$$

where I is the required second moment of area for the belt section.

The maximum possible belt width is defined by the "all-belt" configuration, in which the belt width reaches the span-wide distance between the belts.

These three conditions define the admissible design domain, as shown in Figure 21.

Choosing the maximum belt thickness minimizes the belt width, which leads to the minimum weight condition.

Structural improvement can be achieved by choosing materials with high Young's modulus and/or higher allowed strain. Both widen the design domain (see Figure 22).

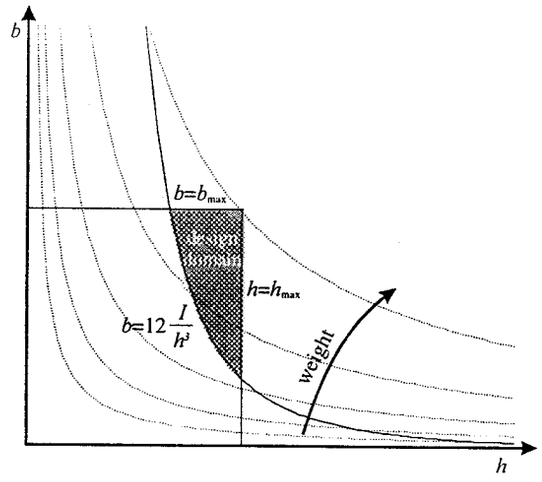

FIGURE 21 - Design curves for the belt's cross section

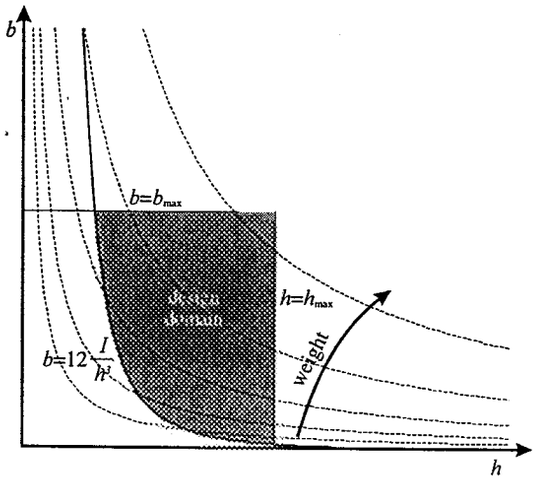

FIGURE 22 - Design curves for the belt's cross section – effect of Young's modulus and maximum allowed strain

The realization of a belt with variable cross section constitutes a further opportunity for structural optimization.

Outlook

The reported numerical and experimental verification of the new flap structure based on the belt-rib concept confirm this as a practicable way for realizing lightweight wing structures with variable camber.

In contrast with the most other concepts which can be found in literature, the belt-rib concept achieves the desired geometrical adaptability purely through structural flexibility: no mechanism with moving parts is required.

The new task of geometrical adaptability does not change the classical, well proven wing structural design beyond measure. In particular, there is no need of opening the skin's profile, and its structural function concerning torsional stiffness is preserved.

Extensive investigations about the optimization opportunities mentioned in the previous section will be the topic of future work. Besides this, experimental tests on more complex models are planned. The 1:2 model of a 500 mm wide flap section with two belt ribs, carbon fiber/epoxy skin and hydraulic actuator was completed just before the publication of this paper and will be extensively tested in the next months.

Further issues to be investigated in future research work are the activation through solid-state actuators as well as the use of integral hinges.

Acknowledgments

This research work was carried out in the framework of the major project "ADIF" (Adaptiver Flügel = Adaptive Wing), in which the German Aerospace Center (DLR) takes part together with the partners Daimler-Benz Aerospace Airbus and Daimler Benz Research.

References

(1) J. H. Renken, 1985, *Mission Adaptive wing camber control systems for transport aircraft*, AIAA 3rd Applied Aerodynamics Conference, AIAA-Paper No. 85-5006

(2) C. A. Marchaj, 1996, *Sail performance, theory and practice*, Sec. 2.9, Adlard Coles Nautical, London

(3) M. O. Hannah, 1930, *Expanding wing for aeroplanes*, US-Patent No. 389,987

(4) H. D. Rocheville, 1932, *Airplane wing*, US-Patent No. 1,846,146

(5) R. W. Cone, 1939, *Airplane wing construction*, US-Patent No. 2,152,029

(6) R. C. Frost, E. W. Gomez, R. W. McAnally, 1981, *Airfoil variable camber device and method*, US-Patent No. 4,247,066

(7) R. Rowarth, 1981, *Variable camber wing*, UK-Patent No. 2059368

(8) M. McKinney, 1982, *Variable camber trailing edge for airfoil*, US-Patent No. 4,312,486

(9) F. D. Statkus, 1982, *Continuous skin, variable camber airfoil edge actuating mechanism*, US-Patent No. 4,351,502

(10) H. Hilbig, H. Wagner, 1984, *Variable wing camber control for civil transport aircraft*, ICAS-84 Conference, ICAS-Paper No. 84-5.2.1

(11) J. Szodruch, 1985, *The influence of camber variation on the aerodynamics of civil transport aircraft*, AIAA 23rd Aerospace Sciences Meeting, AIAA-Paper No. 85-0353

(12) E. Greff, 1990, *The development and design integration of a variable camber wing for long/medium range aircraft*, AIAA Journal, 94, pp. 301-312

(13) J. J. Spillman, 1992, *The use of variable camber to reduce drag, weight and costs of transport aircraft*, Aeronautical Journal, 96, pp. 1-9

(14) H. Ahrendt, D. Heyland, W. Martin, 1997, *Das Leitkonzept "Adaptiver Flügel (ADIF)*, DGLR-Jahrestagung, DGLR-Paper No. JT97-147

(15) E. F. Bruhn, 1958, *Analysis and design of aircraft structures*, Tri-State, Ohio

(16) L. F. Campanile, H. Hanselka, 1997, *Aerodynamisches Bauteil, wie Landeklappe, Tragflügel, Höhen- oder Seitenleitwerk, mit veränderbarer Wölbung*, European Patent (pending) No. 98 103 090.1